Journal of Cancer Research and Clinical Oncology (2019) 145:2457–2468
https://doi.org/10.1007/s00432-019-03003-0

ORIGINAL ARTICLE – CANCER RESEARCH

Wilms tumor-suppressing peptide inhibits proliferation and induces apoptosis of Wilms tumor cells in vitro and in vivo

Wei Zhao[1] · Juan Li[2] · Ping Li[2] · Fei Guo[1] · Pengfei Gao[1] · Junjie Zhang[1] · Zechen Yan[3] · Lei Wang[1] · Da Zhang[1] · Pan Qin[1] · Guoqiang Zhao[4] · Jiaxiang Wang[1]

Received: 22 January 2019 / Accepted: 9 August 2019 / Published online: 28 August 2019

Abstract

Background Our previous study identified a Wilms tumor-suppressing peptide (WTSP) that was upregulated in healthy children, but downregulated in children with Wilms tumor (WT). This study aimed to investigate the effect of WTSP on WT growth in vivo and in vitro.

Methods WTSP was synthesized by solid-phase synthesis of FOMC-protected amino acids. Cell growth curve, cytotoxicity, and apoptosis of WTSP-treated human WT cell line (SK-NEP-1) were determined by cell count, Cell Counting Kit-8 assay, and flow cytometry. The expression of key proteins of four WT-associated signaling pathways was determined by real-time PCR and western blotting. The WT xenograft mouse model was established by the armpit injection of SK-NEP-1 cells. The TUNEL assay was used to detect apoptosis in mouse tumor cells.

Results WTSP inhibited the proliferation of SK-NEP-1 cells in a dose- and time-dependent manner, and it arrested SK-NEP-1 cells in G2/M phase. WTSP-treated cells exhibited a low expression of PCNA and Bcl-2 and high expression of Bax. The expression of β-catenin was markedly changed after WTSP treatment. WTSP-treated mice had significantly smaller tumors than untreated mice.

Conclusion Our findings indicated an anti-tumor effect of WTSP, which is correlated with Wnt/β-catenin pathway. This newly identified peptide may exert a therapeutic effect of WT in the future.

Keywords Wilms tumor · Tumor-suppressing peptide · m/z 6455.5 Da · β-Catenin

Introduction

Wilms tumor (WT) is one of the most common malignancies in children and accounts for 6% of all childhood malignancies and 95% of childhood renal malignancies (Davidoff 2012; Pode-Shakked and Dekel 2011). Wilms tumor cells derive from abnormal kidney stem cells during the mesenchymal epithelial transition (Kalapurakal et al. 2004; Gadd et al. 2012). Tumor stage and age are important factors influencing survival (Dome et al. 2006), and early diagnosis and suitable therapy result in the long-term survival. At present, radical nephrectomy is the primary intervention for WT; adjunct chemotherapy and/or radiotherapy are also beneficial, increasing the long-term survival rate to 90% in children with stage I or II WT and 70–80% in children with stage III or IV WT (Akyüz et al. 2010; Kim and Chung 2006; Neville and Ritchey 2000). However, these therapies have complications that can be serious, including heart failure,

✉ Jiaxiang Wang
jiaxiangwangzzu@126.com

1 Department of Pediatric Surgery, The First Affiliated Hospital of Zhengzhou University, No. 1 East Jianshe Road, Erqi District, Zhengzhou 450000, Henan, China

2 Department of Respiratory Medicine, The First Affiliated Hospital of Zhengzhou University, No. 1 East Jianshe Road, Erqi District, Zhengzhou 450000, Henan, China

3 Department of Urinary Surgery, The First Affiliated Hospital of Zhengzhou University, No. 1 East Jianshe Road, Erqi District, Zhengzhou 450000, Henan, China

4 Department of Microbiology and Immunology, Basic Medical College, Zhengzhou University, No. 100 Kexuedadao Road, Zhongyuan District, Zhengzhou 450001, Henan, China

reproductive dysfunction, and kidney dysfunction (De Graff et al. 1996; Di et al. 2015; Iarussi et al. 2003); some patients even develop severe complications in adulthood (Davenport et al. 2012). Thus, developing new therapeutic strategies for WT is imperative for decreasing medical costs and improving patient outcomes.

Since the promotion of proteomics technology, various technologies have been gradually updated and improved. At present, qualitative and quantitative research on complex protein substances has been studied, which provides a more intuitive standard for clinical diagnosis of certain diseases (Jungblut et al. 1999). In recent years, specific protein markers have been identified in various types of tumors (Gregoriadis et al. 2005). For example, somatostatin is a polypeptide drug used in the treatment of neuroendocrine tumors (Appetecchia and Baldelli 2010; Oberg 2010). These specific protein markers play an important role in the diagnosis and treatment of malignant tumors. In our previous study, a peptide with M/Z of 6455.5 Da was found to be a diagnostic indicator and prognostic factor of WT, with high serum expression in healthy children and low serum expression in children with WT (Wang et al. 2006; Zhang et al. 2009). In addition, the expression of this peptide was increased after radical nephrectomy, reaching near-normal levels, but remained low in patients with partially resected WT or recurrent/metastatic WT (Zhang et al. 2010; Qian et al. 2011). Thus, we speculated that this peptide may influence the occurrence and development of WT. The results of our pilot study showed this peptide inhibited the proliferation of WT cells. Thus, the peptide was named as 'Wilms tumor suppressing peptide' (WTSP).

In the present study, we further investigated the effect of WTSP on WT growth in vitro and in vivo. In addition, we demonstrated that the protective effect of WTSP in WT was partly correlated with Wnt/β-catenin pathway.

Materials and methods

Cell lines and cell culture

Human WT cell line (SK-NEP-1 cells) was purchased from the American Type Culture Collection (ATCC, USA). This cell line grows in suspension and is semi-adherent. The medium was refreshed once every 2–3 days, and cells were passaged once every 7–8 days at 84% McCoy's 5A (modified) medium (GIBCO, USA) containing 15% fetal bovine serum (Qualified, Australia Origin; GIBCO, USA), and 1% penicillin–streptomycin (liquid; GIBCO, USA).

Synthesis of WTSP

Solid-phase synthesis of FOMC-protected amino acids was employed to synthesize WTSP using the LifeTein's PeptideSyn^{TM} technology station, and specific operations were carried out using the LifeTein LLC (New Jersey, USA). The resultant WTSP was a single-stranded peptide (Table 1), and the secondary structure model of this peptide was forecasted and constructed by the molecular modeling server (SWISS-MODEL, Switzerland) (Fig. 1a, b). High-performance liquid chromatography (HPLC) showed its purity was 96.57% (Fig. 2a) and mass spectrometry (MS) identified its characterization (Fig. 2b). At room temperature, WTSP was dissolved in normal saline to prepare 1 μmol/mL WTSP solution, which was then stored at − 20 °C in the dark.

Cell growth curve and doubling time

SK-NEP-1 cells in the logarithmic growth phase were resuspended and added in 24-well plates (400 μL/well with a cell density of 2×10^4 cells/well). Cells were incubated for 1 day and the cells were collected from three wells for cell counting as the initial cell count (day 0). Then WTSP was added to cells at concentrations of 0, 1×10^{-6}, 1×10^{-5},

Table 1 WTSP amino acid sequence and related information

	Sequence interpretation and physiochemical properties of WTSP
Single letter code	DVSSALDKLKEFGNTLEDKARELISRIKQSELSAKMREWFSETFQKVKEKLKIDS
Triple letter code	Asp-Val-Ser-Ser-Ala-Leu-Asp-Lys-Leu-Lys-Glu-Phe-Gly-Asn-Thr-Leu-Glu-Asp-Lys-Ala-Arg-Glu-Leu-Ile-Ser-Arg-Ile-Lys-Gln-Ser-Glu-Leu-Ser-Ala-Lys-Met-Arg-Glu-Trp-Phe-Ser-Glu-Thr-Phe-Gln-Lys-Val-Lys-Glu-Lys-Leu-Lys-Ile-Asp-Ser
Number of residues	55
Molecular weight	6432.41 g/mol
Extinction coefficient	5690 $M^{-1}cm^{-1}$
Iso-electric point	pH = 9.4
Net charge at pH 7	1
Estimated solubility	Good water solubility

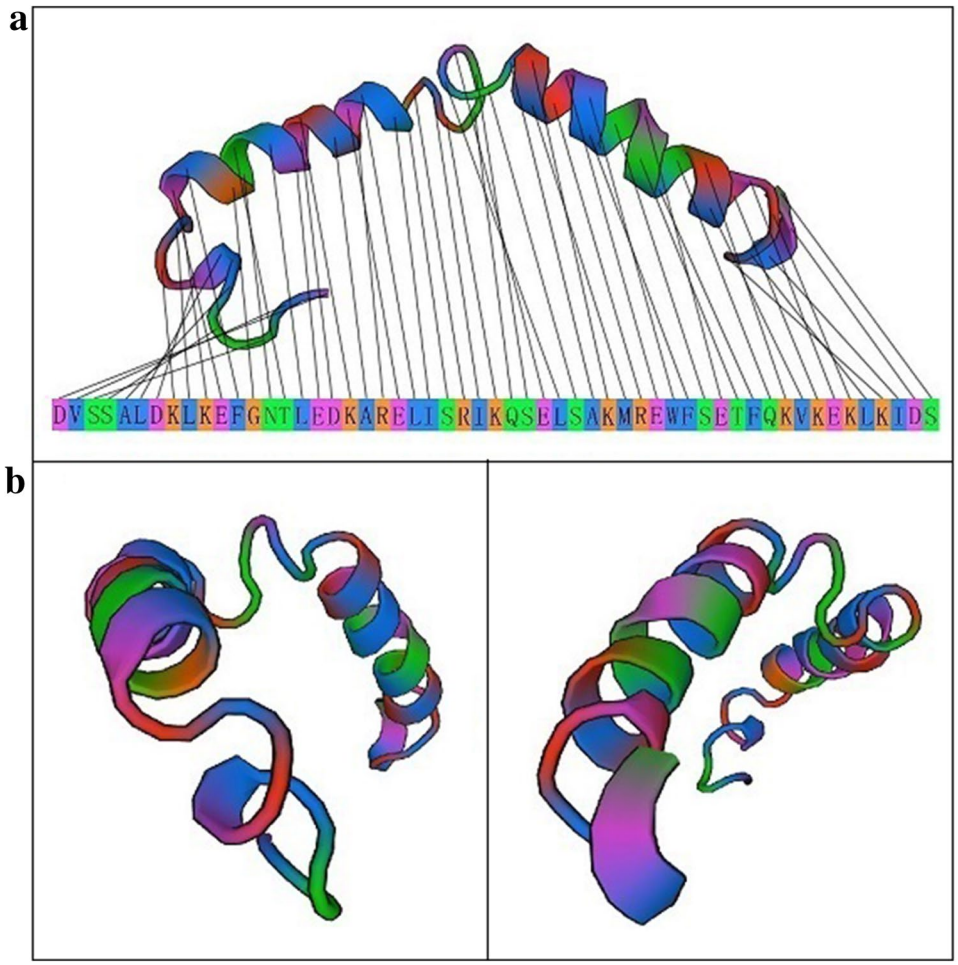

Fig. 1 The secondary structure and the purity of WTSP. **a** The secondary structure model of WTSP was forecasted and established, and the matchup between the sequence and the model was shown. **b** The model of WTSP was viewed from other perspectives

1×10^{-4}, 1×10^{-3} and 1×10^{-2} μmol/mL once. The final volume was 500 μL by adding the incubation medium. Cells treated with normal saline served as the control-treated group. Every 24 h, cells were collected from three wells of the WTSP-treated and saline-treated groups, stained with trypan blue staining, and the viable cells were counted under a light microscope (day 1–7). Then the cell growth curve was conducted. The doubling time was calculated using the Patterson formula: $T_d = T\times\log2/(\log N_t - \log N_o)$. The mean value was calculated from Td3–4, Td3–5, and Td3–6 and presented.

Cytotoxicity of WTSP

SK-NEP-1 cells in the logarithmic growth phase were resuspended and added in 96-well plates (100 μL/well) at a density of 1×10^5 cells/well. After incubation for 1 day, cells were treated with WTSP at different concentrations (0, 0.5, 1.0, 1.5, 2.0, 2.5, and 3.0×10^{-2} μmol/mL). Cells treated with normal saline served as the saline-treated group. After incubation for 24, 48, or 72 h, CCK8 assay (Dojindo, Japan) was performed. Optical density (OD) was measured 2 h later at 450 nm/630 nm, followed by calculation of cell counts and delineation of the cell viability curve. Using this curve, the 50% (IC_{50}) and 80% inhibitory concentrations (IC_{80}) were determined at 24, 48, and 72 h.

Detection of apoptotic and necrotic cells by flow cytometry

SK-NEP-1 cells in the logarithmic growth phase were resuspended and added in 6-well plates (1500 μL/well) at a density of 5×10^4 cells/well. After incubation for 1 day, cells were treated with WTSP at 0, the IC_{50} at 48 h, and the IC_{80} at 48 h. Two days later, cells were harvested and washed twice with cold PBS. After mixing with 100 μL of binding buffer, cells were incubated with annexin-V/PI (BD Biosciences, USA) double staining solution for 15 min at room temperature. The apoptotic or necrotic cells were detected by flow cytometry, and the proportion of apoptotic cells was calculated.

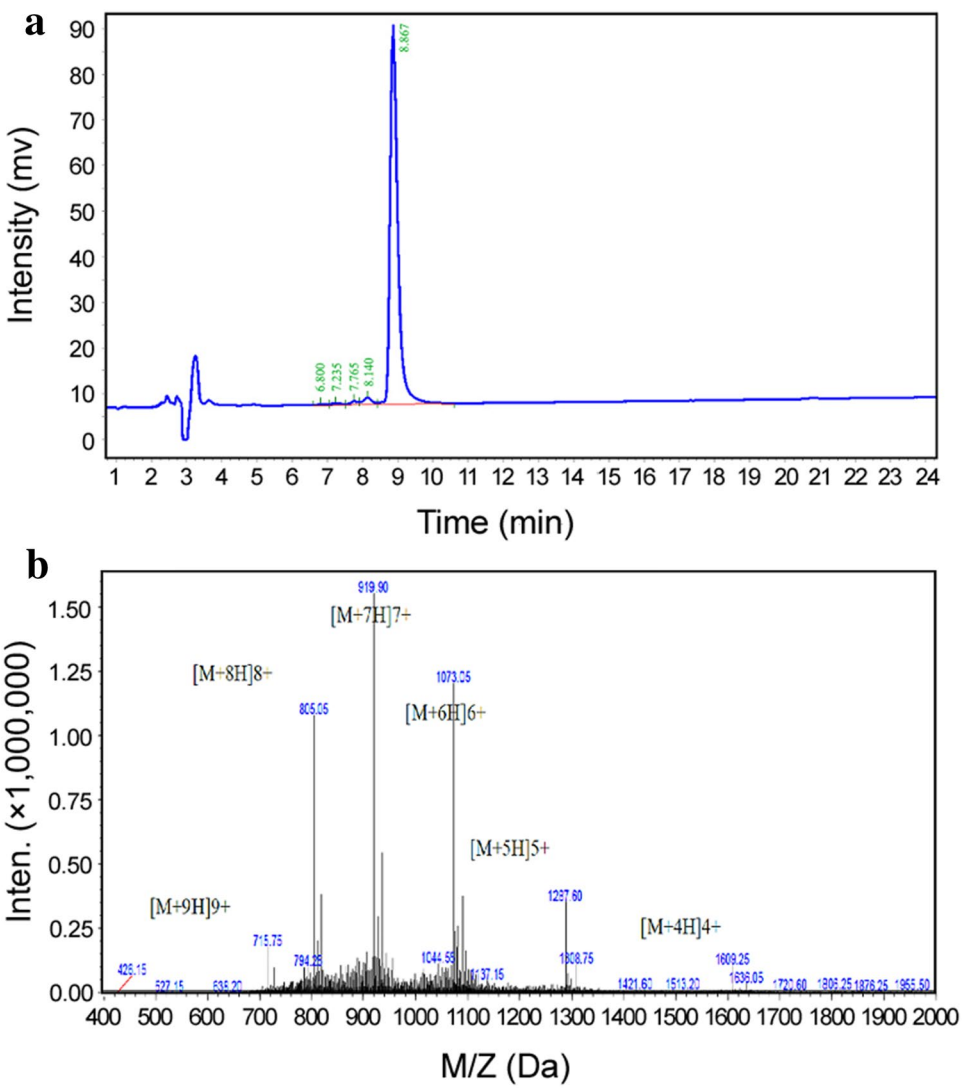

Fig. 2 WTSP was detected by HPLC and MS. **a** After synthesis, WTSP was subjected to HPLC. Pure WTSP was observed at a retention time of 8.867 min; the proportion of this peptide was 96.57%. **b** The evidence of identity based on mass spectral characterization

Determination of cell cycle by flow cytometry

SK-NEP-1 cells in the logarithmic growth phase were re-suspended and added in 6-well plates (1500 µL/well) at a density of 5×10^4 cells/well. After incubation for 1 day, cells were treated with WTSP at 0, the IC_{50} at 48 h, and the IC_{80} at 48 h. Two days later, cells were harvested and washed twice with cold PBS. After mixing with 300 µL of binding buffer, cells were incubated with RNaseA and propidium iodide (PI) for 15 min at room temperature. The proportion of cells in each stage of the cell cycle was determined by flow cytometry.

Reverse transcription-polymerase chain reaction (RT-PCR) and real-time PCR

SK-NEP-1 cells in the logarithmic growth phase were re-suspended and added to 2 25-cm^3 flasks (6 mL/flask) at a density of 5×10^5 cells/mL. After incubation for 1 day, cells were treated with WTSP at 0, the IC_{50} at 48 h, and the IC_{80} at 48 h. Two days later, cells were harvested (5×10^6 cells/group), and total RNA was extracted. The RevertAid First-Strand cDNA Synthesis Kit was used for the synthesis of first-strand cDNA by RT-PCR. After reverse transcription into cDNA, the mRNA expression of PCNA, Bcl-2, Bax, DKK1, DKK2, GSK-3α, GSK-3β, β-catenin, patched, Shh, Smo, TGF-β, Smad1, Smad2, Smad4, Smad5, EGFR, VEGFC, MAPK, AKT, and β-actin was measured by real-time PCR. The primers used for PCR are shown in Table 2, and PCR was carried out using the two-step method as follows: UDG pre-treatment at 50 °C for 2 min, pre-denaturation at 95 °C for 10 min, a total of 40 cycles of denaturation at 95 °C for 15 s, annealing at 60 °C for 30 s, and extension at 60 °C for 30 s. molecular analysis software (Applied Biosystems,7 USA) was used to analyze PCR products, and a standardized method was used to calculate the mRNA expression of target genes normalized to β-actin expression.

Table 2 Real-time PCR primer sequences

Gene	Primer sequence (5′→3′)	
	Forward	Reverse
PCNA	TGGAGAACTTGGAAATGGAA	CGTTGAAGAGAGTGGAGTGG
Bcl-2	ATGTGTGTGGAGAGCGTCAA	GAGACAGCCAGGAGAAATCAA
Bax	CTGGAAGAAGATGGGCTGAG	TGTGTCCCGAAGGAGGTTTA
DKK1	AGCACCTTGGATGGGTATTC	CACACTTGACCTTCTTTCAGGA
DKK2	TTTGCTGTGCTCGTCATTTC	TGGCATCTTTCCATACTTTGC
GSK-3α	GAACTGCGATGTCTGGGAAC	GTGAGGAGGGATGAGAATGG
GSK-3β	AACCGCAGAACCTCTTGTTG	CAGCCAGCAGACCATACATC
β-Catenin	ATGGCAACCAAGAAAGCAAG	TAGCACCTTCAGCACTCTGC
Patched	CATCAACTGGAACGAGGACA	GTGGTGGTGAAGGAAAGCAC
Shh	GCTCGGTGAAAGCAGAGAAC	CCAGGAAAGTGAGGAAGTCG
Smo	TGGGACAGGAAAGAGAGGAA	TTTGAGCCAGACATCCAGAA
TGF-β	CTGGCGATACCTCAGCAAC	TAAGGCGAAAGCCCTCAAT
Smad1	TTACCTGCCTCCTGAAGACC	TCATAAGCAACCGCCTGAAC
Smad2	AGCAGAATACCGAAGGCAGA	TGGGACTTGATTGGTGAAGC
Smad4	CTGCCAACTTTCCCAACATT	ATCCATTCTGCTGCTGTCCT
Smad5	GCTTCTGGCTCAATCTGTCA	GGGTGCTGGTTACATCCTG
EGFR	GCCTTGACTGAGGACAGCAT	GCTTGGACACTGGAGACTGG
VEGFC	GCAGTTACGGTCTGTGTCCA	CTGTCCTTGAGTTGAGGTTGG
MAPK	TTGACAGCAATGGAGAATGG	CCAGAGGAAAGCAACACTGA
AKT	CCTCAAGAATGATGGCACCT	AGGCAGCGGATGATGAAG
β-actin	GTTGCGTTACACCCTTTCTTG	GTCACCTTCACCGTTCCAGT

Western blotting

SK-NEP-1 cells in the logarithmic growth phase were re-suspended and added to 2 75-cm^3 flasks (12 mL/flask) at a density of 5×10^5 cells/mL. After incubation for 1 day, cells were treated with WTSP at 0 and the IC_{50} at 48 h. Two days later, saline-treated cells and WTSP-treated cells were harvested and washed with PBS twice and then lysed in RIPA lysis buffer with PMSF. The Pierce BCA Protein Assay Kit (Thermo Fisher Scientific, USA) was used to determine protein concentrations. Proteins (50 μg) were separated by 12% polyacrylamide gel electrophoresis at 25 mA and then at 90 V for 2 h and transferred onto a PVDF membrane, which was then blocked with 5% nonfat milk for 2 h. The membrane was incubated with antibodies against PCNA (1:1000, rabbit monoclonal antibody, ab92552, Abcam, USA), Bcl-2 (1:1000, rabbit monoclonal antibody, ab185002, Abcam), Bax (1:1000, rabbit monoclonal antibody, ab32503, Abcam), β-catenin (1:5000, rabbit monoclonal antibody, ab32572, Abcam), and β-actin (1:500, mouse monoclonal antibody, ab8226, Abcam) overnight at 4 °C. After washing in TBST, the PVDF membrane was treated with secondary antibody for 2 h and washed with TBST.

Animal xenograft model

The male BALB/c nude mice, aged 4 weeks, were bought from Shanghai Lab Animal Research Center (Shanghai, China). They were housed in a specific pathogen-free environment with a 12-h/12-h dark–light cycle. Procedures were carried out in an aseptic environment. SK-NEP-1 cells were re-suspended in serum containing medium and basement membrane matrix, and the cell density was adjusted to 1×10^7 cell/0.2 mL. After sterilization of the skin, 0.2 mL of SK-NEP-1 cell suspension was injected into the armpit of the forelimb. Two weeks later, when the tumor volume was 125 mm^3, the mice were divided into two groups, receiving intraperitoneal injections for 6 weeks with either WTSP at 4 mg/kg ($n=8$) or normal saline ($n=8$). After 6 weeks, mice were killed, and the volume and the mean diameter of the tumor were measured. The longest diameter (L) and the shortest diameter (S) of the tumor were measured using a vernier caliper. The volume was calculated using the formula πLSS/6. The average diameter is calculated using the formula $(L+S)/2$. All operations were performed under aseptic conditions. All procedures were approved by the Animal Care and Use Committee of Zhengzhou University.

Immunohistochemical analysis

Immunohistochemical analysis was performed using streptavidin-peroxidase conjugated method. The tumors were embedded in paraffin and cut into 4-μm sections, followed by deparaffinization and dehydration. These sections were boiled with 10 mM citrate buffer (pH 6.0) for 10 min for antigen retrieval. Sections were then blocked in 3% H_2O_2 for 10 min to inactivate endogenous peroxidases and treated with normal goat serum (50 μL/section) at room temperature for 20 min to block endogenous biotin. The medium was gently removed, and the sections were incubated with primary antibodies (PCNA, Bcl-2, Bax, and β-catenin, respectively; all 50 μL/section) at 4 °C overnight and then with secondary antibody at 37 °C for 45 min, followed by visualization with peroxidase diaminobenzidine (DAB). Following counterstaining with hematoxylin, the samples were dehydrated using a series of ethanol washes, transparentized with xylene, and mounted using neutral gum.

TUNEL assay

Tumors were fixed in formalin, embedded in paraffin, cut into 4-μm sections, deparaffinized, and dehydrated. After washing in PBS twice, sections were treated with protease K at 37 °C for 15 min and then with 3% hydrogen peroxide for 10 min at room temperature to inactivate endogenous peroxidase. The In Situ Cell Death Detection Kit-POD (Roche, Switzerland) as employed for the detection of apoptotic cells, which were then observed under a fluorescence microscope.

Statistical analysis

The results were presented as the mean ± standard deviation (SD). SPSS version 18.0 (SPSS Inc, Chicago, IL, USA) with a Student's *t* test was used in the statistical analyses. *P* values less than 0.05 were considered statistically significant.

Results

WTSP inhibits the proliferation of SK-NEP-1 cells in vitro

SK-NEP-1 cells were treated with WTSP at different concentrations and the cell growth curve was delineated according to the cell number over the course of 7 days (Fig. 3a). The results showed that the growth rate of WTSP-treated cells was slower than that of saline-treated cells in a dose-dependent. The mean doubling time was calculated from Td3-4, Td3-5, and Td3-6 and presented in Fig. 3b. The doubling time was increased with the enhancement of WTSP concentration. At day 7, the saline-treated cell count was 19.876×10^5 cells, and the mean doubling time was 21.88 ± 2.49 h. At a WTSP concentration of 1×10^{-2} μmol/mL, the day 7 cell count was 2.586×10^5 cells, and the mean doubling time was 67.40 ± 4.87 h.

The CCK-8 cell viability assay was performed to investigate the cytotoxicity of WTSP against SK-NEP-1 cells. The concentration of WTSP was 5, 10, 15, 20, 25, and 30×10^{-3} μmol/ml and the treated time was 24, 48, and 72 h, respectively. The result indicated that the high inhibition rate was positively correlated with the increased WTSP concentration and treated time (Fig. 3c). The IC_{50} and IC_{80} were calculated at 24, 48, and 72 h after WTSP treatment with IC_{50} (at 24 h) 17.934×10^{-3} μmol/ml, IC_{50} (at 48 h) 14.667×10^{-3} μmol/ml, IC_{50} (at 72 h) 12.671×10^{-3} μmol/ml, IC_{80} (at 24 h) 31.660×10^{-3} μmol/ml, IC_{80} (at 48 h) 26.336×10^{-3} μmol/ml, and IC_{80} (at 72 h) 23.087×10^{-3} μmol/ml (Fig. 3d). WTSP significantly inhibited the growth of SK-NEP-1 cells in a dose- and time-dependent manner. In addition, we performed real-time PCR and western blotting to detect the mRNA and protein expression of PCNA, a proliferation-related protein. The results showed that the PCNA mRNA and protein level in WTSP-treated cells was lower than that of saline-treated cells (Fig. 3e).

WTSP-induced apoptosis and necrosis of WT cells

Flow cytometry was performed to detect apoptotic and necrotic SK-NEP-1 cells after WTSP treatment. At 48 h after WTSP treatment, the apoptosis rate of saline-treated cells, 48 h IC_{50} WTSP-treated cells (WTSP at a concentration of 14.667×10^{-3} μmol/ml), and 48 h IC_{80} WTSP-treated cells (WTSP at a concentration of 26.336×10^{-3} μmol/ml) was 8.4%, 22.3%, and 69.6%, respectively (Fig. 4).

To elucidate the effect of WTSP on regulating cell cycle, flow cytometry was used to determine the cell cycle stage of cells treated with saline, IC_{50} WTSP, and IC_{80} WTSP. The duration of the G2/M phase in WTSP-treated cells (14.667×10^{-3} μmol/mL [48 h IC_{50}] and 26.336×10^{-3} μmol/mL [48 h IC_{80}]) was significantly prolonged compared with that of saline-treated cells, suggesting that WTSP arrested SK-NEP-1 cells in the G2/M phase (Table 3).

Signaling pathways associated with WTSP

To confirm the inhibitory effect of WTSP on the proliferation of SK-NEP-1 cells, we determined the mRNA and protein expression of Bcl-2 and Bax (two apoptotic-related genes) in these cells using real-time PCR and western blotting, respectively. The expression of Bcl-2 was lower, but Bax was higher in WTSP-treated cells than in those treated with saline (Fig. 5a, b).

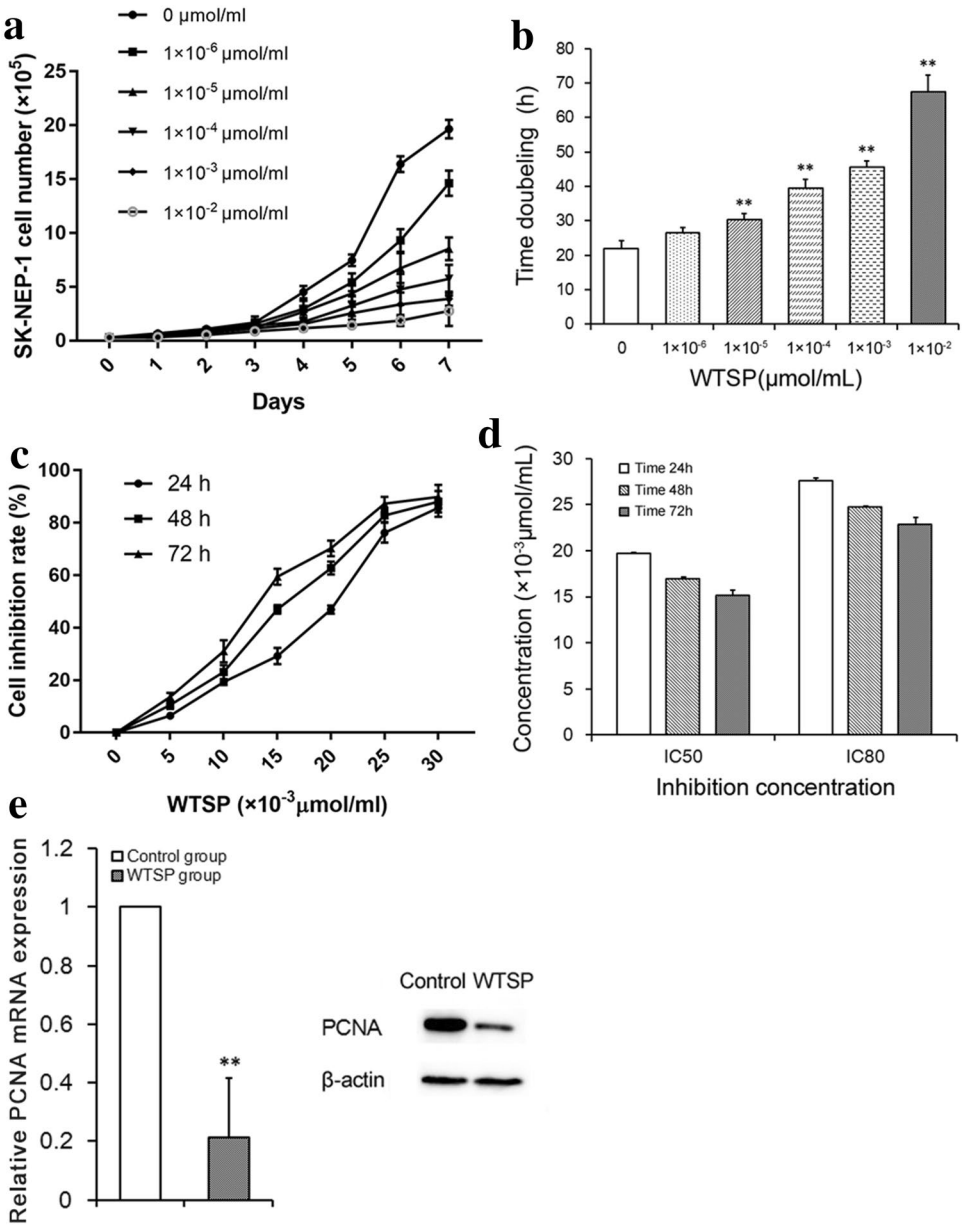

Fig. 3 WTSP inhibits SK-NEP-1 cell proliferation in vitro. **a** The growth curve of SK-NEP-1 cells treated with different concentrations of WTSP (0, 1×10^{-6}, 1×10^{-5}, 1×10^{-4}, 1×10^{-3}, or 1×10^{-2} μmol/mL) for 7 days. **b** Based on the growth curve of WT cells, the doubling times of the cells at different concentrations of WTSP were calculated from Td3-4, Td3-5, and Td3-6 using the Patterson formula. **c** SK-NEP-1 cells (1×10^5 cells/well) were treated with WTSP (0, 0.5, 1.0, 1.5, 2.0, 2.5, or 3.0×10^{-2} μmol/mL) at various time points (24, 48, and 72 h). The cell inhibition rate was determined using a CCK-8 assay. **d** Growth-inhibitory effect of WTSP on SK-NEP-1 cells. The IC_{50} and IC_{80} were calculated at 24, 48, and 72 h after WTSP treatment. **e** Real-time PCR was performed to examine the mRNA expression of PCNA in SK-NEP-1 cells. The protein level of PCNA was determined by western blotting. $^{**}P<0.01$ vs control. Three independent experiments

To explore the mechanism by which WTSP inhibits SK-NEP-1 cell proliferation, we identified four signaling pathways which have been reported to correlate with the pathogenesis of WT, including Wnt pathway (Schweigert et al. 2016), Hedgehog pathway (Oue et al. 2010), TGF-β pathway (Amarante et al. 2017) and growth factor receptor pathway (Li et al. 2008). The expression of the key proteins in these four pathways was detected in the control group and the WTSP group. Real-time PCR was employed to determine the mRNA expression of genes related to the Wnt pathway (DKK1, DKK2, GSK-3α, GSK-3β, and β-catenin), the hedgehog pathway (Patched, Shh, and Smo), TGF-β pathway (TGF-β, Smad1, Smad2, Smad4, and Smad5), and growth factor receptor pathway (EGFR, VEGFC, MAPK and AKT). β-Catenin mRNA expression was significantly lower in WTSP-treated cells than in saline-treated cells ($P<0.05$) (Fig. 5c). In addition, western blotting confirmed the lower β-catenin expression in WTSP-treated cells (Fig. 5b). The above findings suggest the Wnt/β-catenin pathway plays an important role in WTSP-induced inhibition of SK-NEP-1 cell proliferation.

Anti-tumor effect of WTSP in the animal xenograft model

To investigate the anti-tumor effect of WTSP in vivo, a WT-bearing nude mouse model was established. Sixteen nude mice were divided into two groups and treated

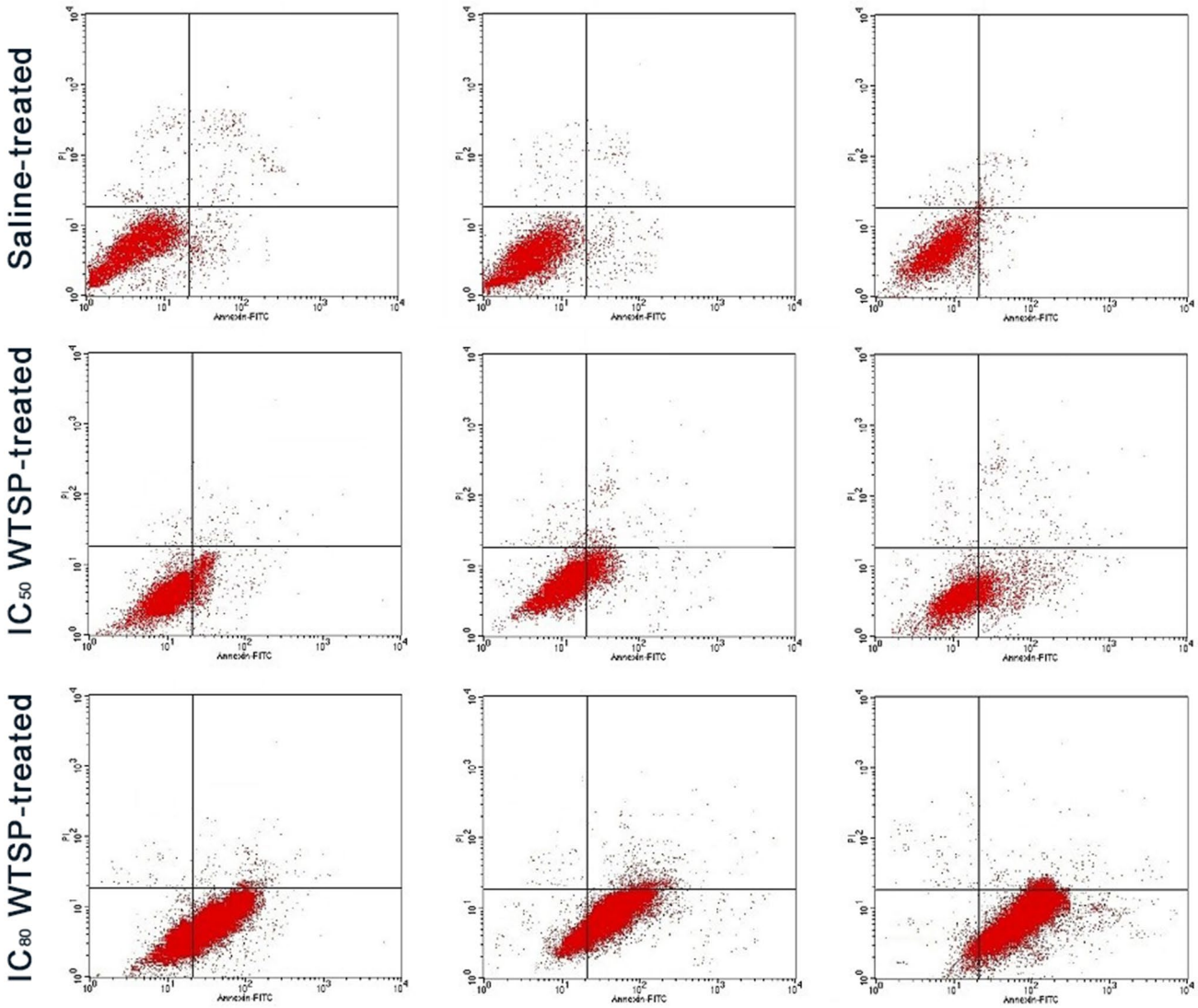

Fig. 4 WTSP induces apoptosis and necrosis of SK-NEP-1 cells in vitro. Flow cytometric analysis of annexin-V/propidium iodide (PI)-stained SK-NEP-1 cells treated with WTSP (IC_{50} and IC_{80}) for 48 h. The dual-parameter dot plots combining annexin-V-fluorescein isothiocyanate (FITC) and PI fluorescence show the following cell populations: lower left quadrant, viable cells (annexin-V−, PI−); lower right quadrant, apoptotic cells (annexin-V+, PI−); upper right quadrant, apoptotic cells (annexin-V+, PI+); and upper left quadrant, necrotic cells (annexin-V−, PI+). Three independent experiments

Table 3 Cell cycle distribution of SK-NEP-1 cells

	G0/G1	G2/M	*S*
Saline-treated group	61.96 ± 1.95	5.63 ± 0.63	32.41 ± 1.49
IC_{50} WTSP-treated group	59.37 ± 2.15	8.70 ± 0.73**	31.96 ± 1.85
IC_{80} WTSP-treated group	57.76 ± 2.65*	9.99 ± 1.00**	32.26 ± 1.99

*$P < 0.05$, **$P < 0.01$ represent statistically significant difference between the WTSP-treated group and saline-treated group

intraperitoneally with either normal saline or WTSP (4 mg/kg) once daily for 6 consecutive weeks. The diameter and volume of tumors after 6 weeks in WTSP-treated mice were significantly smaller than those in control mice (Fig. 6a, b). The harvested tumors were also sectioned and stained with H&E and TUNEL to confirm the anti-tumor effect of WTSP. H&E staining showed normal tumor growth in controls, but massive necrosis and disrupted tissues in tumors from WTSP-treated mice (Fig. 7a). After TUNEL staining, massive apoptotic tumor cells were observed (Fig. 7b). Immunohistochemistry revealed the expression of PCNA, β-catenin, and Bcl-2 was lower and

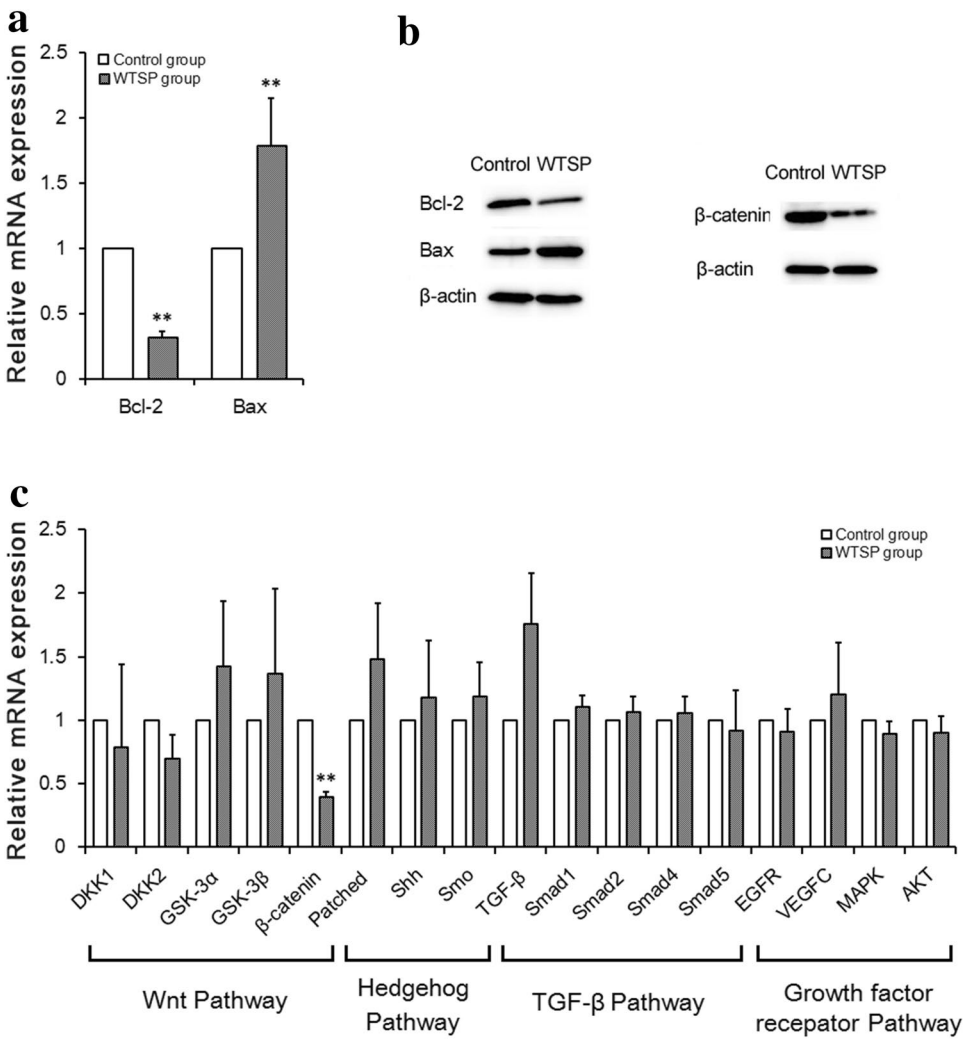

Fig. 5 Signaling pathways affected by WTSP in vitro. **a** The expression of Bax and Bcl-2 was detected by real-time PCR. **b** The protein levels of Bcl-2, Bax, and β-catenin were determined by western blotting. **c** Real-time PCR was performed to examine mRNA expression of members of the Wnt pathway (DKK1, DKK2, GSK-3α, GSK-3β and β-catenin), hedgehog pathway (Patched, Shh and Smo), TGF-β pathway (TGF-β, Smad1, Smad2, Smad4 and Smad5), and growth factor receptor pathways (EGFR, VEGFC, MAPK, and AKT). $^{**}P < 0.01$ vs control. Three independent experiments

Bax expression was higher in tumors from WTSP-treated mice than in control mice (Fig. 7c–e).

Discussion

Our previous study identified a 6455.5 Da polypeptide (WTSP) with the potential to serve as a diagnostic and prognostic factor. In the current study, WTSP inhibited the proliferation of WT cells and made them arrest in G2/M phase in a dose- and time-dependent manner. In addition, WTSP induced cell apoptosis and necrosis of WT cells partly through Wnt/β-catenin-signaling pathway.

PCNA plays an important role in the initiation of cell proliferation and is considered an indicator of cell proliferation (Marjolein et al. 2011). The low PCNA expression observed in our study suggests the proliferation of WT cells was inhibited by WTSP. Proteins in the Bcl2 family, such as Bcl-2 and Bax, play a critical role in cell apoptosis. Bcl-2 is a negative regulator of cell apoptosis, increasing the resistance of cells to external stimulation and cytotoxin-induced death (Paunesku et al. 2001). In contrast to Bcl-2, Bax is a positive regulator of cell apoptosis and plays a pro-apoptotic role (Korsmeyer 1995). In WTSP-treated cells, Bcl-2 expression was low and Bax expression was high, suggesting WTSP induced WT cell apoptosis partly through combating cytotoxins. Consistent with these in vitro findings, immunohistochemistry of tumor samples from WTSP-treated nude mice revealed low PCNA expression, low Bcl-2 expression, and high Bax expression. Together, these findings indicated that WTSP can effectively inhibit the proliferation of WT cells and induce their apoptosis and necrosis.

Several tumor inhibitory peptides have been developed into anti-tumor drugs. For example, somatostatin is a polypeptide drug used in the treatment of neuroendocrine tumors (Appetecchia and Baldelli 2010; Oberg 2010). Studies on cancer proteomics showed that breast cancer has a high HER2 expression, leading to the design of a specific peptide drug targeting HER2. Such peptide can bind to HER2, forming lytic polypeptide polymers that

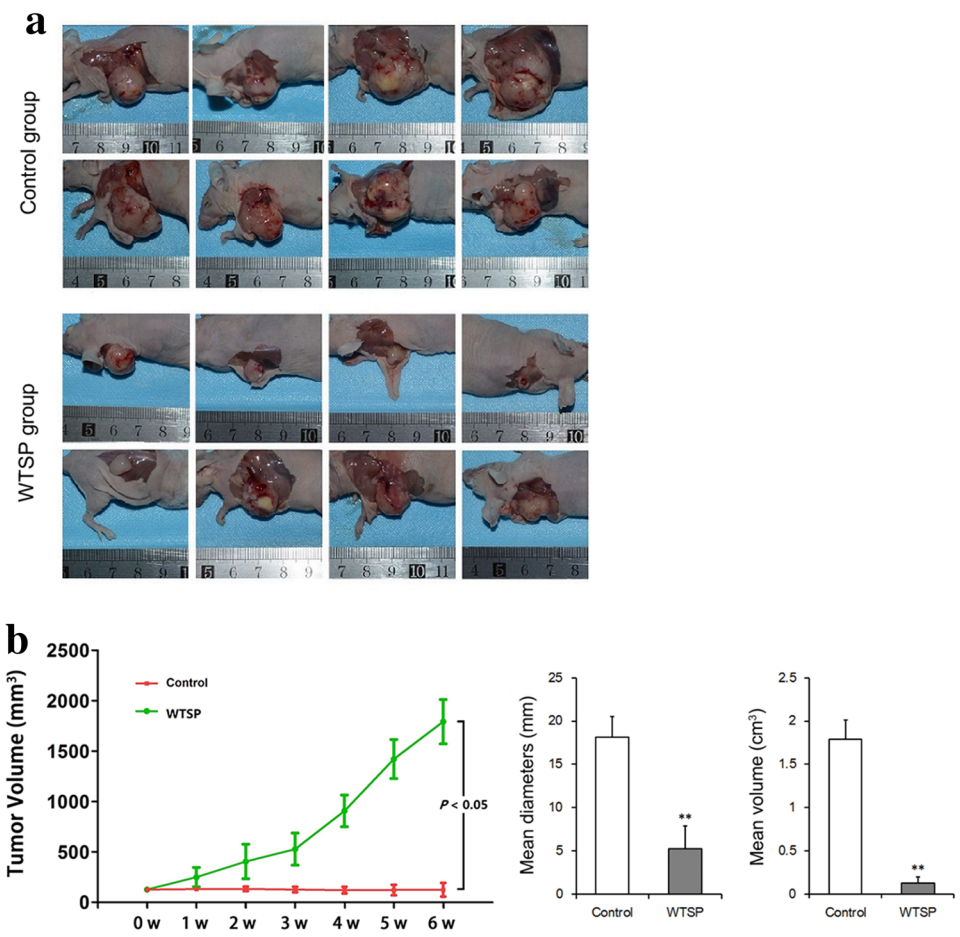

Fig. 6 WTSP inhibited WT growth in vivo. **a** Gross observation of SK-NEP-1 subcutaneous tumors in nude mice from the control group ($n=8$) and the WTSP group ($n=8$) (4 mg/kg). **b** The mean diameter and volume of tumors from the start of WTSP treatment. $^{**}P<0.01$ vs control

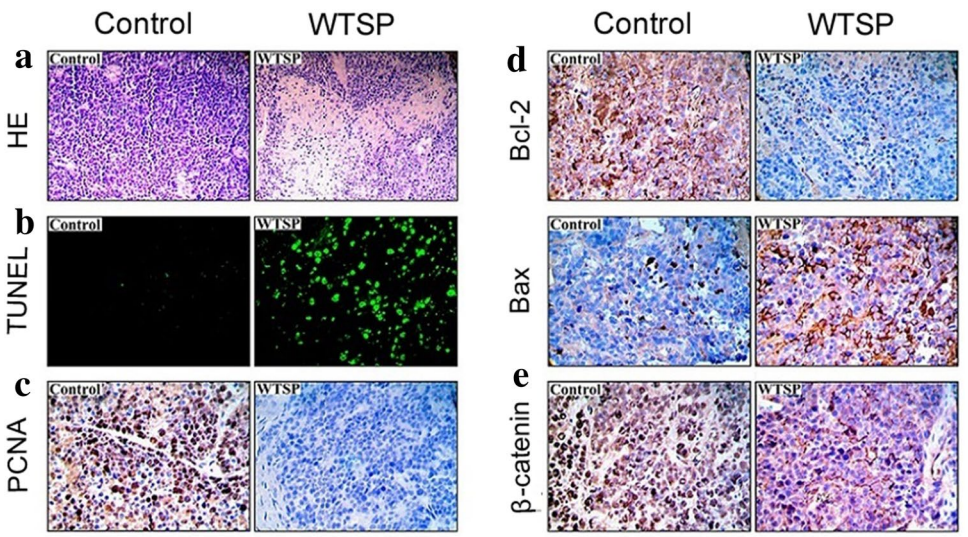

Fig. 7 Anti-tumor effect of WTSP in vivo. **a** H&E staining. Magnification, 10×10. **b** TUNEL assay indicated increased apoptosis in WTSP-treated tumor tissue. Magnification, 20×10. **c** Immunohistochemistry analysis of PCNA. Magnification, 20×10. **d** Immunohistochemistry analysis of Bcl-2 and Bax. Magnification, 20×10. **e** Immunohistochemistry analysis of β-catenin. Magnification, 20×10. Three independent experiments

are potently cytotoxic against breast cancer cells without affecting normal cells. The therapeutic effect of this peptide in breast cancer is superior to that of trastuzumab and lapatinib (Kawamoto et al. 2013). Scientists in Germany have designed a bifunctional peptide that can bind to a kidney cancer-specific WNT signaling protein receptor to form polypeptide polymers that exert anti-cancer effects on kidney cancer cells without affecting normal cells (Koller et al. 2013; Karoline et al. 2013). Tumor inhibitory peptide is an endogenous, 20-amino-acid protein that can affect the

physiological and biochemical processes of bacteria and viruses. The therapeutic use of tumor inhibitory peptides has many advantages over other chemotherapeutic agents. Children with WT usually develop repeated congestive heart failure during chemotherapy with doxorubicin-based protocols (Green et al. 2001) or develop metabolic syndrome after radiotherapy (Antonsson 2001). Tumor inhibitory peptide has the advantageous properties of endogenous proteins, including low toxicity, high efficiency, high specificity, and a low propensity to accumulate in humans. Thus, the development of a polypeptide that targets WT cells has been the goal of many studies on cancer proteomics. The half-life and the characteristics of WTSP in serum are definitely important for the newly defined peptide, which will be further investigated in our future researches.

Our investigations of the mechanism underlying WTSP-induced apoptosis showed that WTSP down-regulates the expression of β-catenin, a key component in the Wnt signaling pathway. Encoded by the *CTNNB1* gene, β-catenin is a key factor that regulates cell proliferation and gene mutation. The role of Wnt/β-catenin in the etiology and pathogenesis of cancers is still controversial (Logan and Nusse 2004). Several investigations have found that Wnt/β-catenin (CTNNB1) plays an important role in the pathogenesis of WT (Clark et al. 2011). The down-regulation of β-catenin expression observed in WTSP-treated WT cells in our work may be responsible for WTSP-induced apoptosis of WT cells. Recently, some regulatory non-coding RNAs have been demonstrated to regulate gene expressions. Maybe the dysregulation of a specific non-coding RNA results in the down-regulation of WTSP in WT patients. Meanwhile, higher serum level of WTSP may also participate in the normal physiological activities in healthy people. Elucidation of the detailed mechanism underlying the action of WTSP on WT cells requires further investigation.

Body weight is a critical indicator for tumor therapeutic effect. However, the Wilms tumor developed very quickly after the inoculation of tumor cells in the xenografts. The volume and weight of tumor were growing fast due to the high malignancy. As shown in Fig. 6c, the smaller one was as the size of mouse head, and the larger one was bigger than 1/3 of mouse body. Commonly, the mouse weight should be significantly increased after the treatment. However, in our study, the mouse weight in the WTSP-treated and WTSP-untreated groups appeared no significant changes as the tumor grew too fast. Therefore, tumor volume and diameter were compared between the two groups. New methods to evaluate body weight deserve further investigations in the future researches.

Taken together, our data demonstrate that WTSP is an anti-tumor peptide that induces apoptosis and inhibits proliferation of WT cells partly through down-regulation of β-catenin, which may provide a novel strategy for the treatment of WT.

Acknowledgements The study was conducted within the Department of Pediatric Surgery supported by the First Affiliated Hospital of Zhengzhou University. The study was financially supported by the National Natural Science Foundation of China (81172085, 81071782). We thank all of the patients participating in the study.

Author contributions JW and WZ carried out the experiments design, theoretical simulations and data analysis. WZ and JL carried out test operation in animal experiment and cell experiment. PL carried out measurements. WZ and JL wrote the manuscript. ZY, LW and JZ revised the manuscript. DZ, PQ, FG, PG and GZ gave scientific advices. All the authors contributed through scientific discussion and reviewed the manuscript.

Compliance with ethical standards

Conflict of interest We declare that we do not have any commercial or associative interest that represents a conflict of interest in connection with the work submitted.

References

Akyüz C, Yalçin B, Yildiz I et al (2010) Treatment of Wilms tumor: a report from the Turkish Pediatric Oncology Group (TPOG). J Pediatr Urol 6(3):S59–S60

Amarante MK, de Oliveira CEC, Ariza CB, Sakaguchi AY, Ishibashi CM, Watanabe MAE (2017) The predictive value of transforming growth factor-β in Wilms tumor immunopathogenesis. Int Rev Immunol 36(4):233–239

Antonsson B (2001) Bax and other pro-apoptotic Bcl-2 family "killer-proteins" and their victim the mitochondrion. Cell Tissue Res 306(3):347–361

Appetecchia M, Baldelli R (2010) Somatostatin analogues in the treatment of gastroenteropancreatic neuroendocrine tumours, current aspects and new perspectives. J Exp Clin Cancer Res 29(1):19

Clark PE, Polosukhina D, Love H et al (2011) β-Catenin and K-RAS synergize to form primitive renal epithelial tumors with features of epithelial Wilms' tumors. Am J Pathol 179(6):3045–3055

Davenport KP, Blanco FC, Sandler AD (2012) Pediatric malignancies: neuroblastoma, Wilm's tumor, hepatoblastoma, rhabdomyosarcoma, and sacroccygeal teratoma. Surg Clin N Am 92(3):745–767

Davidoff AM (2012) Wilms' tumor. Adv Pediatr 59(1):247–267

De Graff SS, Van Gent H, Reitsma-Bierens WC, Van Luyk WH, Dolsma WV, Postma A (1996) Renal function after unilateral nephrectomy for Wilms' tumour: the influence of radiation therapy. Eur J Cancer 32A(3):465–469

Di TM, Casale F, Indolfi P et al (2015) Compensatory hypertrophy and progressive renal damage in children nephrectomized for Wilms' Tumor. Pediatr Blood Cancer 26(5):325–328

Dome JS, Cotton CA, Perlman EJ et al (2006) Treatment of anaplastic histology Wilms' tumor: results from the fifth National Wilms' Tumor Study. J Clin Oncol 24(15):2352–2358

Gadd S, Huff V, Huang CC et al (2012) Clinically relevant subsets identified by gene expression patterns support a revised ontogenic model of Wilms tumor: a Children's Oncology Group Study. Neoplasia 14(8):742 **(IN720–756, IN721)**

Green DM, Grigoriev YA, Nan B et al (2001) Congestive heart failure after treatment for Wilms' tumor: a report from the National Wilms' Tumor Study Group. J Clin Oncol 19(7):1926–1934

Gregoriadis G, Jain S, Papaioannou I, Laing P (2005) Improving the therapeutic efficacy of peptides and proteins: a role for polysialic acids. Int J Pharm 300(1):125–130

Iarussi D, Indolfi P, Pisacane C et al (2003) Comparison of left ventricular function by echocardiogram in patients with Wilms' tumor treated with anthracyclines versus those not so treated. Am J Cardiol 92(3):359–361

Jungblut PR, Zimny-Arndt U, Zeindl-Eberhart E et al (1999) Proteomics in human disease: cancer, heart and infectious diseases. Electrophoresis 20(10):2100–2110

Kalapurakal JA, Dome JS, Perlman EJ et al (2004) Management of Wilms' tumour: current practice and future goals. Lancet Oncol 5(1):37–46

Karoline M, Young K, Sebastian F et al (2013) Targeting cancer with a bi-functional peptide: in vitro and in vivo results. Vivo 27(4):431–442

Kawamoto M, Horibe T, Kohno M, Kawakami K (2013) HER2-targeted hybrid peptide that blocks HER2 tyrosine kinase disintegrates cancer cell membrane and inhibits tumor growth in vivo. Mol Cancer Ther 12(4):384–393

Kim S, Chung DH (2006) Pediatric solid malignancies: neuroblastoma and Wilms' Tumor. Surg Clin N Am 86(2):469–487

Koller CM, Young K, Schmidt-Wolf IGH (2013) Targeting renal cancer with a combination of WNT inhibitors and a bi-functional peptide. Anticancer Res 33(6):2435–2440

Korsmeyer SJ (1995) BCL-2 gene family and the regulation of programmed cell death. Cold Spring Harbor Symp Quant Biol 59(3):387

Li M-H, Sanchez T, Pappalardo A, Lynch KR, Hla T, Ferrer F (2008) Induction of antiproliferative connective tissue growth factor expression in Wilms' tumor cells by sphingosine-1-phosphate receptor 2. Mol Cancer Res 6(10):1649–1656

Logan CY, Nusse R (2004) The Wnt signaling pathway in development and disease. Annu Rev Cell Dev Biol 20(1):781–810

Marjolein VW, Neggers SJCMM, Hein R, Rij CM, Van Rob P, Heuvel-Eibrink MM, Van Den (2011) Abdominal radiotherapy: a major determinant of metabolic syndrome in nephroblastoma and neuroblastoma survivors. PLoS One 7(12):52

Neville HL, Ritchey ML (2000) Wilms' tumor: overview of National Wilms' Tumor Study Group results. Urol Clin N Am 27(3):435–442

Oberg K (2010) Cancer: antitumor effects of octreotide LAR, a somatostatin analog. Nat Rev Endocrinol 6(4):188

Oue T, Yoneda A, Uehara S, Yamanaka H, Fukuzawa M (2010) Increased expression of the hedgehog signaling pathway in pediatric solid malignancies. J Pediatr Surg 45(2):387–392

Paunesku T, Mittal S, Protić M et al (2001) Proliferating cell nuclear antigen (PCNA): ringmaster of the genome. Int J Radiat Biol 77(10):1007–1021

Pode-Shakked N, Dekel B (2011) Wilms tumor—a renal stem cell malignancy? Pediatr Nephrol 26(9):1535–1543

Qian Z, Jiaxiang W, Rui D, Shaobo Y, Shu Z (2011) Identification of novel serum biomarkers in child nephroblastoma using proteomics technology. Mol Biol Rep 38(1):631–638

Schweigert A, Fischer C, Mayr D, von Schweinitz D, Kappler R, Hubertus J (2016) Activation of the Wnt/β-catenin pathway is common in wilms tumor, but rarely through β-catenin mutation and APC promoter methylation. Pediatr Surg Int 32(12):1141–1146

Wang JX, Zhang J, Liu QL, Wang L, Fan YZ, Jie-Kai YU (2006) Detecting biomarkers from serum in nephroblastoma patients with support vector machine. Zhonghua Yi Xue Za Zhi 86(42):2982

Zhang B, Wang J, Yu J, Zheng S (2009) A serum protein fingerprint in the diagnosis and prognosis of Wilms' tumors in children. Life Sci J 6(1):27–32

Zhang Q, Yan S et al (2010) Detection of biomarkers in children with Wilms' tumor using proteinchip technology. Chin Med J 123(14):1939